Planetary and Space Science 81 (2013) 82–85

Contents lists available at SciVerse ScienceDirect

Planetary and Space Science

journal homepage: www.elsevier.com/locate/pss

Where did the Luna 23 and 24 spacecraft land?: Comparing the spacecraft seen in LROC NAC images with synthetic images

V.P. Dolgopolov [a], A.T. Basilevsky [b,*], M.S. Robinson [c], J.B. Plescia [d], J.W. Head [e]

[a] Lavochkin Association, 24 Leningradskaya Street, Khimki, Moscow region 141400, Russia
[b] Vernadsky Institute of Geochemistry and Analytical Chemistry, Russian Academy of Sciences, Moscow 19991, Russia
[c] School of Earth and Space Exploration, Box 871404, Arizona State University, Tempe, AZ 85287-1404, United States
[d] The Johns Hopkins University, Applied Physics Laboratory, 11100 Johns Hopkins Road, MS 200-W230, Laurel, MD 20723, United States
[e] Department of Geological Sciences, Brown University, Providence, RI 02912, United States

ARTICLE INFO

Article history:
Received 12 March 2013
Received in revised form
29 March 2013
Accepted 30 March 2013
Available online 9 April 2013

Keywords:
The Moon
Luna 23
Luna 24

ABSTRACT

Shkuratov et al. (2013) described specific photometric anomalies found around the Luna 16, 20 and 23 spacecraft and not found around the Luna 24 spacecraft. The authors explained this lack of an anomaly at the Luna 24 site as a result of the misidentification of the Luna 23 and 24 spacecraft in the LROC images by Robinson et al. (2012). In order to address this question, we synthesized images of the Luna spacecraft as they might appear in the LROC images (made by the Lavochkin Association, builders of the Luna spacecraft series). We compared the model images of the virtual Luna 23 and Luna 24 spacecraft sitting on the lunar surface with the spacecraft seen in the LROC images and concluded, on the basis of similarity of the spacecraft seen in the LROC images with the synthetic images, that identification of the spacecraft in these images by Robinson et al. (2012) is likely correct.

1. Introduction

Shkuratov et al. (2013) recently published a paper in which they analyzed Lunar Reconnaissance Orbiter Narrow Angle Camera (LROC NAC; Robinson et al., 2010) images of the landing sites of Luna 16, 20, 23 and 24. Ratios of NAC images acquired of each site with varying phase angles revealed distinct soil disturbances attributed to impingement of the rocket plume on the surface during landing. The photometric anomalies found around the Luna 16, 20 and 23 spacecraft were distinctly similar, while that of the Luna 24 spacecraft was located 150 m NW of the spacecraft. Shkuratov et al. (2012) proposed that the photometric anomalies were caused by rocket engine gas jets smoothing out the surface "by destroying the primordial 'fairy castle' structure that effectively produces the shadow-hiding effect". They concluded that the lack of photometric anomaly adjacent to the Luna 24 vehicle is due to a misidentification of the Luna 23 and 24 spacecraft by Robinson et al. (2012).

The Luna 16, 20 and 24 spacecraft successfully landed on the Moon, took samples of lunar soil and delivered them to Earth. The mission of Luna 23 was unsuccessful: at the final stage of descent, the Luna 23 doppler landing device, designed to measure velocity and distance, failed. As a result, at an altitude of 130 m the measurement of spacecraft altitude stopped and the spacecraft reached the surface in an abnormal regime: its vertical velocity was 11 m/s instead of 5 m/s, and the landing occurred with the spacecraft inclined by 10–15°. As a result the spacecraft overturned onto its side where the drilling device was located, and this led to spacecraft mechanical damage, depressurization of its instrument module, and the failure of the decimeter radio transmitter. An attempt was made by commands from Earth to activate the soil sampler and to prepare the ascent module for liftoff, but without result, as confirmed by transmissions from the return rocket radio (http://www.laspace.ru/rus/luna23.html).

Shkuratov et al. (2012) concluded that Robinson et al. (2012) misidentified the Luna 23 and 24 landing sites because the proposed Luna 24 vehicle is not coincident with a photometric anomaly and the fact that the Luna 23 vehicle made a hard landing. "*All Apollo and Luna landers are located within their corresponding engine-jet features that are clearly seen with phase-ratio imagery. One exception is the alleged landing site of the Luna-24 probe, which is shifted 150 m to the southeast of the feature. The Luna-24 descent module worked in the regular mode that could not allow for such a shift. A possible explanation is that the sites of the failed Luna-23 and successful Luna-24 landing sites are misidentified, since they are located within each other's area of uncertainty. We suggest that because of incorrect processing of the radar system measuring distance, speed, and lateral drift, the incorrectly governed engine of Luna- 23 resulted in a rebound before they were switched*

* Corresponding author. Tel.: +7 499 137 4995; fax: +7 495 938 2054.
E-mail addresses: atbas@geokhi.ru, Alexander_Basilevsky@Brown.edu (A.T. Basilevsky).

0032-0633/$ - see front matter © 2013 Elsevier Ltd. All rights reserved.
http://dx.doi.org/10.1016/j.pss.2013.03.013

off that resulted in the lander traveling an additional 150 m laterally before coming to a hard landing Shkuratov et al. (2013)."

2. Analysis of NAC images and synthetic images

The correct understanding of the position of the Luna 24 lander on the surface of the Moon is important for a thorough interpretation of the results of the laboratory studies of the samples delivered by this mission. To clarify which vehicle is Luna 23 and which is Luna 24, we synthesized images of the basic Luna vehicle with and without its ascent stage still attached, in various orientations, and compared these images to the NAC images of the actual vehicles resting on the surface. The synthetic images were illuminated under lighting conditions that existed when the LROC images were acquired (solar azimuth 106.8°, Sun 49.5° above the horizon (Fig. 1)).

The spacecraft height from the surface to the top of the return capsule is 4.15 m (Polishchuk and Pichkhadze, 2010). The lander height after the ascent module lifted off is 2.4 m. The diagonal distance between the external edges of the plates of the legs is 4.9 m. The diagonal distance between the external edges of the fuel tanks of the landing module is 2.85 m. It is important to note also that the spacecraft, except for its legs, antenna of the altimeter, and the girder of the drilling device were covered with the 3-cm layer of thermal insulation similar in appearance to white fiberglass fabric. In Fig. 1 the model images are shown without the thermal insulation layer while in the LROC images the spacecraft are seen covered with the thermal insulation. In the case of Luna 24 it is thought that the thermal insulation was partly torn away by the jet of the ascent module rocket (Robinson et al., 2012; see below).

The angular size of the pixel projected to the surface of the LROC images that we analyzed was 29 cm, but was smeared down-track

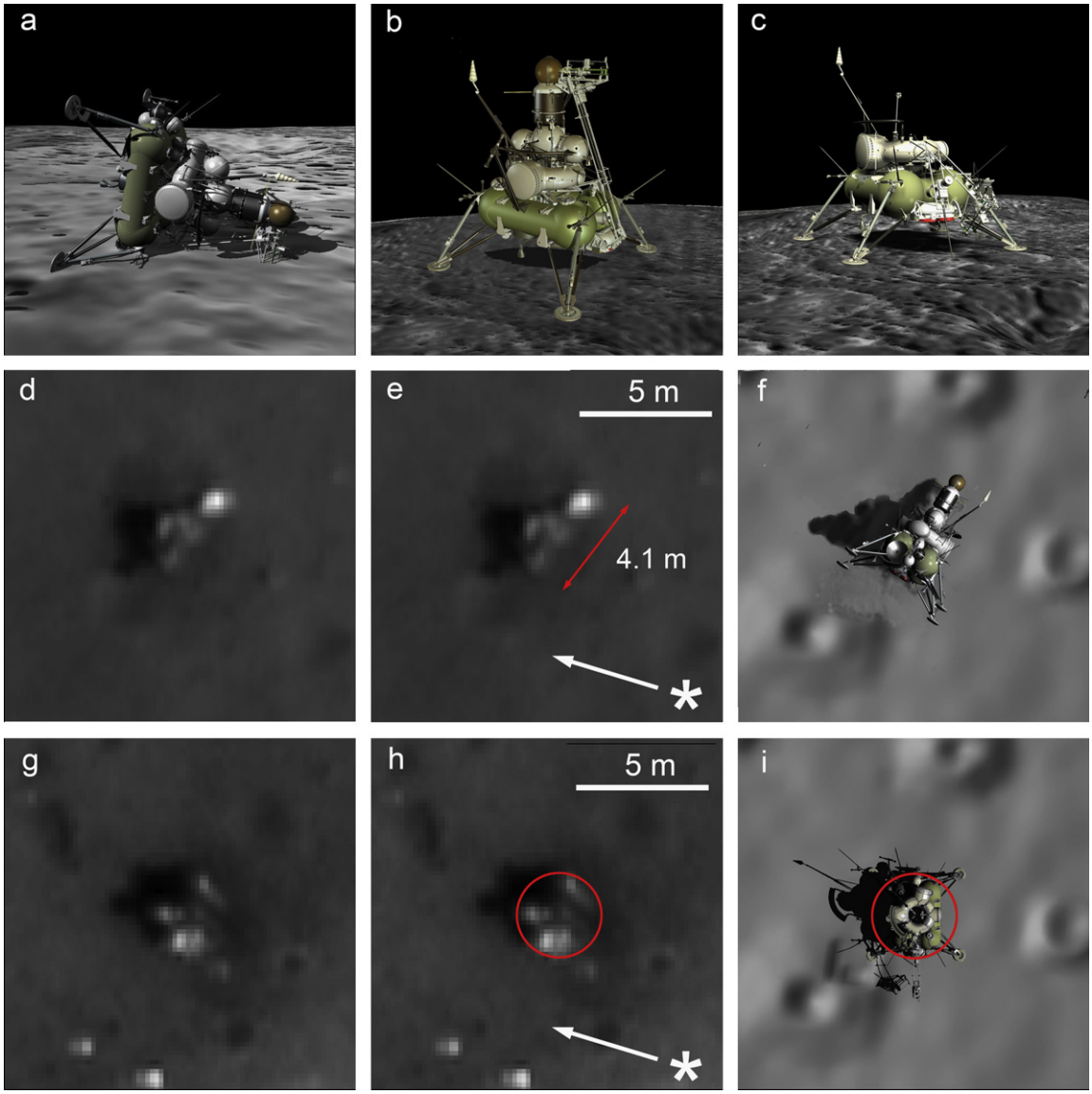

Fig. 1. Model images of the Luna 23 and 24 spacecraft and the LROC NAC images of the spacecraft sitting on the lunar surface: (a) model image of Luna 23 spacecraft overturned at landing with ascent module not separated, view from the side; (b) model image of Luna 24 spacecraft after successful landing, view from the side; (c) model image of Luna 24 spacecraft after liftoff of the ascent module with the capsule containing lunar samples, view from the side; (d) Luna 23 spacecraft seen in LROC NAC M174868307R; (e) the same with direction of solar illumination shown and apparent length of the spacecraft (the two-ended red arrow); (f) model image of the overturned Luna 23 spacecraft taken at the same illumination conditions, view from above; (g) Luna 24 spacecraft seen in LROC NAC M174868307L; (h) the same with direction of solar illumination shown and red circle outlined connecting parts of the spacecraft visible in the image; and (i) model image of the Luna 24 spacecraft, view from above, with the red circle of the same size as in (h). (For interpretation of the references to color in this figure caption, the reader is referred to the web version of this article.)

to 59 cm (Robinson et al., 2010). The image was reprojected with a pixel size of 25 cm into cartographic space, and then this image was expanded to 8 cm pixels to match the higher resolution of the model image. This resampling scheme aids in morphologic analysis relative to the synthetic images. Measurements of the spacecraft are of course limited by the original pixel scale of the unsampled image.

3. Luna 23

The spacecraft which Robinson et al. (2012) considered to be Luna 23, but Shkuratov et al. (2013) considered as Luna 24, is shown in Fig. 1d. The spacecraft shadow is seen to the left, and the visible parts of the spacecraft are bright relative to the regolith (~twice as reflective as the Moon). In Fig. 1e, superposed on the background of the image shown in Fig. 1d, is shown the solar illumination direction. It is seen that the left part of the spacecraft produces relatively long shadows, while in the upper right part of the image are observed short shadows. Taking into account that the Sun was 49.5° above the horizon, measurements of the shadow lengths show that the upper edge of the shadow-producing left part of the spacecraft is about 3 m above the surface, while the extreme right part, not producing a resolvable shadow, rests on the surface. These shadow relations suggest that the spacecraft lies on its side (see Fig. 1a). We conclude that this orientation is consistent with the interpretation of Robinson et al. (2012) that this spacecraft is indeed Luna 23. A model image (view from above) of the recumbent spacecraft is shown in Fig. 1f. It is seen that the shadow in the LROC images (d and e) only approximately match with the model (f) that may be due to surface relief of this place. As described above, the "standing" spacecraft is 4.15 m tall, so the red two-ended arrow in Fig. 1f should be of that size. The length of it measured in Fig. 1e is ~4.1 m that is in good agreement with the spacecraft size.

4. Luna 24

The spacecraft that Robinson et al. (2012) consider as Luna 24, but Shkuratov et al. (2013) interpret as Luna 23, is seen in Fig. 1g. The spacecraft shadow is seen to its left and parts of the spacecraft are also about twice as reflective as typical local regolith. There are more than 15 bright ($>5\times$ average regolith) small spots are seen within several tens of meters around the spacecraft (Robinson et al., 2012). The features do not produce shadows and were proposed to be pieces of thermal insulation material torn away from the landing module by the jet of the ascent module engine (Robinson et al., 2012).

In Fig. 1h (superposed on the background of the image shown in Fig. 1g) are shown the solar illumination direction. The shadows (in the illumination direction) are of approximately the same length 2–3 m, on average 2.5 m; taking into account that the Sun is 49.5° above the horizon suggests that the upper edge of the shadow-producing left part of the spacecraft stands about 3 m above the lunar surface. It is known that the upper part of the landing module after the ascent module lifted off stands above the surface by 2.4 m. This measurement of the spacecraft height on the image is in satisfactory agreement with the known spacecraft size, even taking into account the challenges of measurement constraint for features near or smaller than the pixel size. This conclusion, as well as the fact that the shadow lengths do not vary significantly, suggest that the spacecraft stands on the surface in the nominal position, consistent with the orientation of the Luna 24 spacecraft.

The red circle (3.2 m diameter) in Fig. 1h links the parts of the spacecraft visible in the image. Fig. 1i shows a model of the lander without the ascent module. As described above, the diagonal distance from the external edge of the leg plate to the external edge of the opposite leg plate is 4.9 m, while the diagonal distance between the external edges of the opposite fuel tanks is 2.85 m. If one places here the 3.2 m red circle from Fig. 1h, then it is apparent that it circumscribes the main body of the spacecraft and parts of the legs that were covered by the thermal insulation; consistent with the LROC image of Luna 24 (as identified by Robinson et al., 2012).

5. Discussion and conclusions

In summary, we synthesized images of the Luna 23 and Luna 24 spacecraft sitting on the lunar surface guided by what is seen in LROC images M174868307R and M174868307L; on the basis of these comparisons, we conclude that the identification of the spacecraft in these images by Robinson et al. (2012) was correct. The logic of that original identification was essentially geological: The upper part of the lunar sample core brought by Luna 24 was represented by immature regolith (e.g., Barsukov et al., 1977), while early works on remote sensing of this region suggested some disagreement between these data and the composition of the Luna 24 material (e.g., Pieters et al., 1976). So, from the two spacecraft seen in the LROC images, one sitting on the rim of morphologically very fresh 65-m crater (Robinson et al., 2012; Basilevsky and Head, 2012) and another one sitting in 35 m from the moderately fresh 12-m crater, the first one was considered to be Luna 24 and the second one—Luna 23. An additional argument in favor of the conclusion that the second spacecraft is Luna 23 was that in LROC images it appeared to be a recumbent spacecraft with its ascent module not separated (see Figure 9 in Robinson et al., 2012). The comparisons with the model images described in our analysis appear to confirm this similarity.

It remains enigmatic as to why the photometric anomaly associated with Luna 24 is not observed in the immediate vicinity of the spacecraft (it occurs 150 m NW from the spacecraft) (Shkuratov et al., 2013). Absence of the photometric anomaly in the immediate vicinity of the Luna 24 spacecraft may be due to immature soil at this location. Coarse-grained soils on the rim of the very fresh 65-m crater probably do not exhibit the "fairy castle" structure, so the engine jet impact did not encounter or destroy this structure and thus the anomaly was not formed. It cannot be excluded, however, that the observed photometric anomaly 150 m NW of Luna 24 was caused by the jet of the main engine of the Luna 24 spacecraft; in this scenario, after transition to the deceleration by the small engines, the spacecraft translated horizontally 150 m SE, and successfully landed away from the anomaly. The absence of the anomaly caused by the jet of the engine of the Luna 24 ascending module in this case may be explained by the immaturity of the regolith on the rim of the fresh crater previously mentioned.

In conclusion, the correct understanding of the position of the Luna 24 lander on the surface of the Moon is important for the comprehensive interpretation of results of laboratory studies of the samples delivered by this mission. Based on the above consideration we conclude that identification of the Luna 23 and 24 spacecraft by Robinson et al. (2012) is correct. Further acquisition of new LROC NAC images will provide additional information on the nature of the Luna landing sites and the state of the remaining spacecraft.

Acknowledgments

Authors are grateful to A.V. Ivanov, O.N. Zaitseva A.G. Meister and R. Wagner for help in this work, interpretation of the images and useful discussions.

References

Barsukov V.L., Tarasov L.S., Dmitriev L.V., Kolesov G.M., Shevaleevsky I.D., Garanin A. V., 1977. The geochemical and petrochemical features of regolith and rocks from Mare Crisium (preliminary data). In: Proceedings of 8th Lunar Science Conference, pp. 3319–3332.

Basilevsky, A.T., Head, J.W., 2012. Age of Giordano Bruno crater as deduced from the morphology of its secondaries at the Luna 24 landing site. Planetary and Space Science 73, 302–309.

Pieters, C., McCord, T., Adams, J.B., 1976. Regional basalt types in the Luna 24 landing area as derived from remote observations. Geophysical Research Letters 3 (11), 697–700.

Polishchuk G.M. and Pichkhadze K.M., 2010. Robotic spacecraft for fundamental and applied scientific studies. MAI Print. 659 p. (in Russian).

Robinson, M.S., Plescia, J.B., Jolliff, B.L., Lawrence, S.J., 2012. Soviet lunar sample return missions: landing site identification and geologic context. Planetary and Space Science, 69; 76–88.

Robinson, M.S., Brylow S.M., Tschimmel M., Humm D., Lawrence S.J., Thomas P.C., Denevi B.W., Bowman-Cisneros E., Zerr J., Ravine M.A., Caplinger M.A., Ghaemi F.T., Schaffner J.A., Malin M.C., Mahanti P. Bartels A., Anderson J., Tran T.N., Eliason E.M., McEwen A.S., Turtle E., Jolliff B.L., Hiesinger H., 2010. Lunar Reconnaissance Orbiter Camera (LROC) Instrument Overview. Space Science Reviews, http://dx.doi.org/10.1007/s11214-010-9634-2.

Shkuratov, Yu., Kaydash, V., Sysolyatina, X., Razim, A., Videen, G., 2013. Lunar surface traces of engine jets of Soviet sample return probes: the enigma of the Luna-23 and Luna-24 landing sites. Planetary and Space Science 75, 28–36.